

Search for magnetic monopoles and nuclearites with the ANTARES experiment

Gabriela Emilia Păvălaș, for the ANTARES Collaboration

Institute of Space Science, Bucharest-Magurele, RO-077125

Abstract

We report on the search for magnetic monopoles and nuclearites with the ANTARES experiment, using data collected in 2007 and 2008. Both magnetic monopoles and nuclearites are expected to produce a large signal inside the detector. The analysis of data yielded no exotic candidates, and upper limits were set on the flux of fast upgoing magnetic monopoles and of slow downgoing nuclearites.

Keywords: magnetic monopoles, nuclearites, neutrino telescope

1. Introduction

ANTARES is a detector designed for neutrino astronomy, that can also contribute to the search for hypothetical massive particles [1, 2], such as magnetic monopoles [3, 4] and nuclearites [5]. Magnetic monopoles were initially predicted by Dirac in 1931, in order to explain the quantization of the electric charge. They were rediscovered almost 40 years later by 't Hooft and Polyakov, as a natural occurrence in GUT theories. Since then, monopoles were intensively searched for in various experimental facilities, like MACRO [6], Baikal [7], AMANDA-II [8], but no such particle was detected. Nuclearites are hypothetical lumps of strange quark matter, that may be present in the cosmic radiation. The most representative upper limit on the nuclearite flux, for the mass range expected at the ANTARES depth, was that established by MACRO [9]. In this paper, dedicated analyses and their results for relativistic magnetic monopoles and slow nuclearites are presented for 116 and 310 active days, respectively.

2. The ANTARES detector

ANTARES is located in the Mediterranean Sea, at 2475 m depth, 40 km south of Toulon [10]. It is an array of 885 optical modules (OMs), arranged in triplets on 12 lines anchored to the sea bed. An OM consists of a glass sphere housing a 10" Hamamatsu photomultiplier (PMT). Each line is connected to the main junction box, which is linked to the shore station. Until the completion with 12 lines in mid-2008, ANTARES took data in partial configurations of 5 lines (2007), 9 and 10 lines (2008).

The data acquisition system sends to shore all PMT signals above a pre-defined threshold, typically 0.3 photoelectrons (pe) [11]. Then the raw signals are filtered by various triggers and stored. The time and charge information of the PMT signals is digitized into "hits", labeled L0 hits. The standard algorithms used to identify muon

events are based on local coincidences. A local coincidence (or L1 hit) is defined either as two L0 hits on the same storey, within 20 ns, or as a single hit with a large charge, usually above either 3 or 10 pe threshold.

The muon triggers used are the so-called directional trigger (DT), operational both in 2007 and 2008, and the cluster trigger (CT), implemented since 2008. DT requires at least 5 L1 hits correlated in space and time, while CT looks for a pair of clusters of two L1 hits in 2 out of 3 consecutive storeys, within a $2.2 \mu s$ time window, the characteristic time of a relativistic particle to cross the detector.

Both analyses presented in this article are using a blinding strategy. This requires the definition and optimization of the selection criteria using Monte Carlo simulations and the validation of the simulations on a fraction ($\sim 15\%$) of the available data.

3. Magnetic monopoles

According to Grand Unified Theories (GUT), magnetic monopoles may have formed in the early Universe. It was shown by 't Hooft [12] and Polyakov [13] that they appear as a result of the spontaneous breaking of a semi-simple gauge group that contains the $U(1)_{E.M.}$ subgroup. Their magnetic charge g is defined as a multiple integer of the Dirac charge $g_D = \hbar c/2e$, where e is the elementary electric charge, \hbar the Planck's constant and c the speed of light.

Fast monopoles can lose a large amount of energy in the terrestrial environment. Nevertheless, magnetic monopoles with mass below $\sim 10^{14}$ GeV could be accelerated to relativistic velocities by cosmic magnetic fields, and thus could reach the ANTARES detector from below.

3.1. Magnetic monopole signal in water

Depending on the velocity, the light signal can be produced either as direct Cherenkov emission, for magnetic

monopoles with $\beta > 0.74$ or as indirect Cherenkov emission, for $\beta > 0.51$, by means of the knock-out electrons (δ -rays) pulled out from the atoms by the magnetic monopole. Thus, a monopole with one Dirac charge may emit about 8500 more photons than a muon with the same velocity, as shown in Fig. 1.

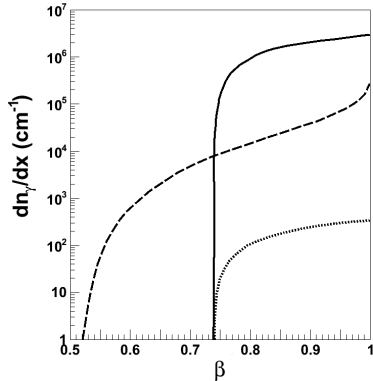


Figure 1: Expected light yield in the 300-600 nm wavelength range in sea water from magnetic monopoles with unit Dirac charge (solid line), from δ -rays produced along the monopole path (dashed line) and from muons (dotted line), as a function of velocity.

3.2. Magnetic monopole analysis

For this analysis, data taken in 2008 with 9, 10 and 12 line configurations were used, with a total livetime of 136 days. Upgoing magnetic monopoles were simulated for 10 velocity ranges within $\beta=[0.550,0.995]$. Monte Carlo upgoing atmospheric neutrinos and downgoing atmospheric muons were considered for background. The simulated events were processed using the active triggers, along with the dead channel information and the optical background rates extracted from a group of experimental runs for each detector configuration.

In order to account for the different velocities of simulated monopoles, one of the ANTARES track reconstruction algorithms [14] was modified by implementing the velocity as a free parameter and by optimizing it for the crossing of magnetic monopoles [4]. This algorithm is based on the minimization of the time residuals using the least square method, with a very stringent hit selection. The Gaussian resolution obtained for the reconstructed monopole velocity is $\sigma_\beta \sim 0.003$ for $\beta > 0.8$ and $\sigma_\beta \sim 0.03$ for lower velocities.

Both MC events and a 15% data sample (~ 20 days active time) have been reconstructed with the modified algorithm. Then data-MC comparisons were performed using various parameters and preliminary cuts were defined. These cuts require events with reconstructed $\beta > 0.60$ and zenith angle $< 90^\circ$.

For the final event selection, discriminative variables were defined. The first discriminative variable is the number of hits used in the reconstruction, n_{hit} . A data-MC

comparison of the n_{hit} distributions is shown in Fig. 2. The second variable is the so-called λ parameter, defined as the logarithmic ratio between the track quality factors $Q_t(\beta_{rec} = 1)$ and $Q_t(\beta_{rec} = \text{free})$, obtained from the standard muon reconstruction and from the modified reconstruction, respectively. The quality factor is the sum over the number of hits of squared time residuals plus an adjusting term for distant hits with large charge. The cut parameter space (n_{hit}, λ) defined for every region of reconstructed velocities was optimized by minimizing the Model Discovery Factor for a 5σ discovery at 90% probability.

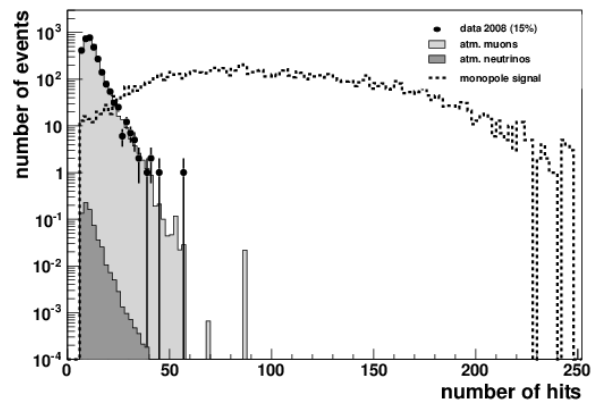


Figure 2: Distribution of the number of hits for MC magnetic monopoles (dashed line) reconstructed with $\beta_{rec} = [0.775, 0.825]$. Comparisons of simulated atmospheric downgoing muons (light gray) and upgoing neutrinos (medium gray) with 15% data samples (solid dots) are also shown.

4. Results

After unblinding, a very good data-MC agreement is obtained for the remaining 85% of data. The final results obtained after applying the selection cuts on the unblinded data are shown in Table 1.

β_{rec} range	# of expected background events	# of observed events	90% C.L. flux upper limit ($\text{cm}^{-2} \text{s}^{-1} \text{sr}^{-1}$)
[0.625, 0.675]	2.2×10^{-2}	0	7.5×10^{-17}
[0.675, 0.725]	1.3×10^{-1}	1	8.9×10^{-17}
[0.725, 0.775]	4.6×10^{-2}	0	4.0×10^{-17}
[0.775, 0.825]	1.1×10^{-6}	0	2.4×10^{-17}
[0.825, 0.875]	8.2×10^{-7}	0	1.8×10^{-17}
[0.875, 0.925]	6.9×10^{-7}	0	1.7×10^{-17}
[0.925, 0.975]	2.3×10^{-5}	0	1.6×10^{-17}
[0.975, 1.025]	1.3×10^{-2}	0	1.3×10^{-17}

Table 1: For each velocity range of monopoles, the number of expected and observed events, and the 90% C.L. upper limits for the 85% of the unblinded data are given.

One event survived the selection cuts in the interval $\beta_{rec}=[0.675, 0.725]$. Given the expected background of 0.13, which requires five events for a 5σ deviation, the observation is compatible with the background-only hypothesis.

The Feldman-Cousins 90% C.L. upper limit obtained for this interval considers the observed event as background [4]. The upper flux limit for upgoing magnetic monopoles, obtained for 116 days of ANTARES data (corresponding to 85% of the unblinded data), is shown in Fig. 3. This is the most stringent upper limit for upgoing magnetic monopoles in the velocity range $0.625 < \beta < 0.995$ ($\gamma=10$) [4].

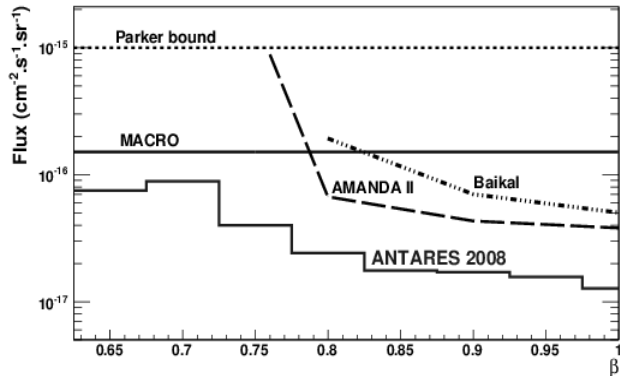


Figure 3: The preliminary ANTARES 90% C.L. upper limit for upgoing magnetic monopoles, compared to the upper limits set by MACRO, Baikal and AMANDA II, and the theoretical Parker bound [15].

5. Nuclearites

Nuclearites are hypothetical massive particles of up, down and strange quarks in approximately equal proportions. They may have formed in the early Universe [16], or in high energy astrophysical phenomena, like supernovae and strange star collisions [17]. Their velocity is assumed to be $\beta \simeq 10^{-3}$, the typical velocity of gravitationally trapped objects inside the galaxy. Nuclearites with masses larger than $\sim 3 \times 10^{13}$ GeV could reach the ANTARES depth from above and could be detected by means of the black-body radiation from their overheated path in the traversed medium [18].

5.1. Nuclearite signal in water

Nuclearites would interact through elastic collisions with the atoms of the medium, with an energy loss: $dE/dx = -\sigma\rho v^2$, where σ represents the interaction cross section of the nuclearite, ρ the density of the medium, and v the velocity of the particle [18]. The cross section values are $\sigma = \pi \times 10^{-16}$ cm² for nuclearite masses $M \leq 8.4 \times 10^{14}$ GeV, and $\pi(3M_N/4\pi\rho_N)^{2/3}$ cm² for larger masses [18].

In water, an estimated fraction $\eta \simeq 3 \times 10^{-5}$ of the energy loss is released as black body radiation in the visible range [18]. The number of visible photons per unit path length can be computed from the relation: $dN_\gamma/dx = \eta dE/\langle E \rangle dx$, where the mean energy of visible photons is assumed to be $\langle E \rangle \simeq \pi$ eV.

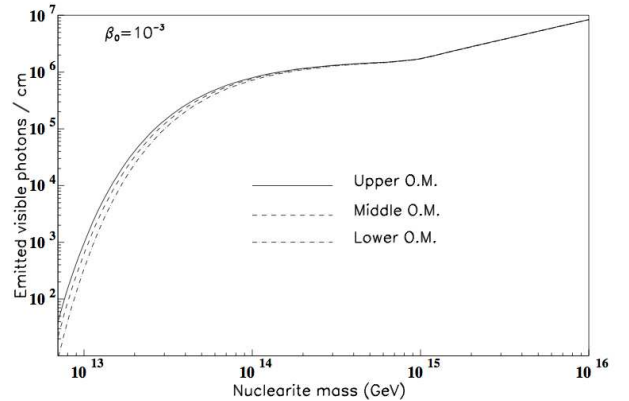


Figure 4: Number of photons per unit path length emitted by vertically downgoing nuclearites, at depths corresponding to different storeys of an ANTARES string.

The light yield expected from nuclearites is shown in Fig. 4. The number of visible photons emitted by vertically downgoing nuclearites can be orders of magnitude higher than the number of Cherenkov photons emitted by a muon with $\beta \sim 1$ (see for comparison Fig. 1).

5.2. Analysis

In this analysis, we considered data taken during 2007 and 2008, with various detector configurations. These configurations are defined by the number of active lines, the triggers used, and the high threshold on the charge of L1 hits, the latter depending on bioluminescence activity. The total livetime amounts to 310 days.

A dedicated Monte Carlo program was developed for the simulation of nuclearites. A hemispherical simulation volume of 548 m radius centered on the detector axis is considered, as well as isotropic directions of the tracks from above the detector. Nuclearites were simulated in the mass range $3 \times 10^{13} - 10^{17}$ GeV, with an initial velocity outside the Earth atmosphere of $\beta = 10^{-3}$. At the ANTARES depth, the dominant background for nuclearites is caused by the downgoing atmospheric muons. The muons were simulated with the MUPAGE code [19]. The simulated nuclearites and muons were processed using the triggers described in Section 2 and by adding background extracted from a group of experimental runs for each configuration.

5.2.1. Selection conditions

Characteristic of the nuclearite signal is the long duration of the event inside the detector (about 1 ms) compared to the typical duration of a muon event (about 2.2 μ s). When a muon event is triggered, all hits are recorded in an enlarged snapshot containing 2.2 μ s before and after the cluster of L1 hits, while a typical nuclearite event will produce a sequence of multiple enlarged snapshots within 1 ms.

The discriminative variable used for the nuclearite signal selection is the snapshot duration dt , defined as the time difference between the last and the first L1 hit that

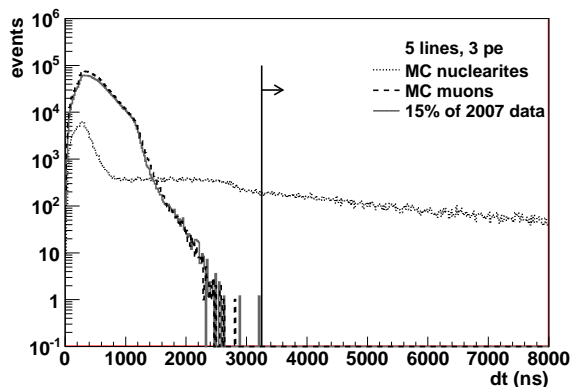


Figure 5: Comparison between simulated nuclearites (dotted line), simulated muons (dashed line) and a 15% data sample (solid grey line) as a function of the snapshot duration dt , for the 5 line configuration, with a 3 pe high threshold. The vertical line represents the optimized C1 cut.

produce a trigger. Comparisons of dt distributions for simulated nuclearites and muons were performed for every detector configuration, and optimized cuts were established by minimizing the upper flux limits obtainable if no signal is found. As an example, the dt distributions of simulated nuclearites, muons and a 15% data sample, for the 5 line configuration, together with the optimized cut, are presented in Fig. 5.

The C1 cuts were applied on 15% of data from every detector configuration, and 11 events remained. For each of these events, the time evolution of the charge barycenter was studied. Because the light emitted by nuclearites is isotropic, the charge barycenter indicates the position of the source at a certain moment. All data events were consistent with stationary light sources, attributed to short term (\sim hundreds of milliseconds) bioluminescence bursts.

In order to reduce the bioluminescence background, a second level (C2) cut was introduced. This cut requires either events with multiple snapshots within 1 ms or single snapshot events with a duration larger than twice the value of the C1 cut. After applying the C2 cuts, no event in the 15% data samples survived.

6. Results

Once the data were unblinded, they were filtered by applying the corresponding cuts. Seven events from the 9 line configuration survived the cuts. Their topology investigation, using the charge barycenter vs time distributions, revealed no downgoing tracks; three of them were due to sparking OMs and the other four were products of bioluminescence bursts, thus they were not considered in calculating the limit. The Feldman-Cousins 90% C.L. upper limit for a flux of downgoing nuclearites was computed for 310 days of data from 2007 and 2008. The preliminary ANTARES limit is presented in Fig. 6, and compared with the MACRO [9] and SLIM [20] limits.

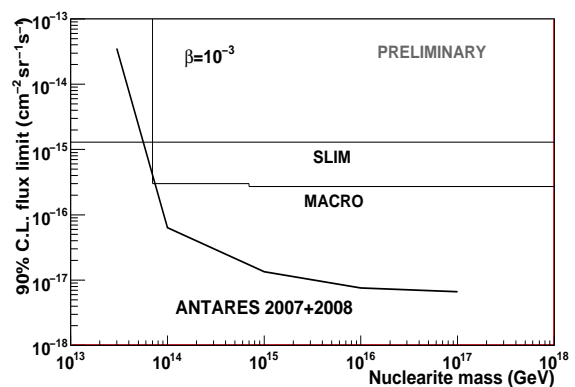


Figure 6: The ANTARES 90% C.L. upper limit for a flux of downgoing nuclearites, for 310 days of data collected during 2007 and 2008. The limits obtained by MACRO and SLIM are also shown.

7. Conclusions

The first results of the searches for relativistic magnetic monopoles and slow nuclearites with the complete ANTARES detector were presented. The ANTARES upper flux limit for upgoing magnetic monopoles in the velocity range $0.625 < \beta < 0.995$ is the most stringent up to date. The upper limit for a flux of downgoing nuclearites improves the MACRO result and is the best present limit for the nuclearite mass range $10^{14} - 10^{17}$ GeV.

Acknowledgements. This work was partially supported by UEFISCDI, under contract 32/2011.

References

- [1] V. Popa, for the ANTARES Coll., Nucl. Instrum. Meth. A 567 (2006) 480
- [2] G. Pavlas, N. Picot Clemente, Proceedings of the 31st ICRC, Lodz, 2009, arXiv:0908.0860
- [3] N. Picot Clemente, Proceedings of the 32nd ICRC, Beijing, 2011, arXiv:1112.0478
- [4] S. Adrian-Martinez et al. (ANTARES Coll.), Astropart. Phys. (2012), doi: 10.1016/j.astropartphys.2012.02.007
- [5] V. Popa, Proceedings of the 32nd ICRC, Beijing, 2011, arXiv:1112.0478
- [6] M. Ambrosio et al. (MACRO Coll.), Eur. Phys. J. C 25 (2002) 511
- [7] V. Aynutdinov et al. (BAIKAL Coll.), Astropart. Phys. 29 (2008) 366
- [8] R. Abbasi et al. (IceCube Coll), Eur. Phys. J. C 69 (2010) 361
- [9] M. Ambrosio et al. (MACRO Coll.), Eur. Phys. J. C 57 (2008) 525
- [10] J.A. Aguilar et al. (ANTARES Coll.), Nucl. Instrum. Meth. A 656 (2011), 11-38, arXiv : 1104.1607
- [11] J.A. Aguilar et al. (ANTARES Coll.), Nucl. Instrum. Meth. A 570 (2007) 107
- [12] G. 't Hooft, Nucl. Phys. B 79 (1974) 276
- [13] A.M. Polyakov, Sov. Phys. JETP Lett. 20 (1974) 194
- [14] J.A. Aguilar et al. (ANTARES Coll.), Astropart. Phys. 34 (2011) 652
- [15] E.N. Parker, Astrophys. J. 160 (1970) 383
- [16] E. Witten, Phys. Rev. D 30 (1984) 272
- [17] J. Madsen, Phys. Rev. D 71, 014026 (2008)
- [18] A. De Rújula, S.L. Glashow, Nature 312 (1984) 734
- [19] G. Carminati et al., Comput. Phys. Commun. 179 (2008) 915
- [20] S.Cecchini et al., Eur. Phys. J. C 57 (2008) 525